

# Experimental and theoretical investigation of temperature-dependent electrical fatigue studies on 1-3 type piezocomposites

Cite as: AIP Advances 6, 035311 (2016); <https://doi.org/10.1063/1.4944582>

Submitted: 20 December 2015 . Accepted: 07 March 2016 . Published Online: 21 March 2016

Y. Mohan, and A. Arockiarajan

## COLLECTIONS

Paper published as part of the special topic on [Chemical Physics](#), [Energy, Fluids and Plasmas](#), [Materials Science](#) and [Mathematical Physics](#)



View Online



Export Citation



CrossMark

## ARTICLES YOU MAY BE INTERESTED IN

[Modeling of dielectric and piezoelectric response of 1-3 type piezocomposites](#)

Journal of Applied Physics **112**, 044107 (2012); <https://doi.org/10.1063/1.4748057>

[Effect of viscoelastic and dielectric relaxing matrix on ferroelastic behaviour of 1-3 piezocomposites](#)

AIP Advances **5**, 027103 (2015); <https://doi.org/10.1063/1.4907767>

[Viscoelastic modeling and experimental characterization of thermo-electromechanical response of 1-3 piezocomposites](#)

Journal of Applied Physics **116**, 214103 (2014); <https://doi.org/10.1063/1.4903287>



## NEW: TOPIC ALERTS

Explore the latest discoveries in your field of research

[SIGN UP TODAY!](#)

## Experimental and theoretical investigation of temperature-dependent electrical fatigue studies on 1-3 type piezocomposites

Y. Mohan<sup>a</sup> and A. Arockiarajan<sup>b</sup>

*Dept. of Applied Mechanics, Indian Institute of Technology Madras, Chennai, India-600036*

(Received 20 December 2015; accepted 7 March 2016; published online 21 March 2016)

1-3 type piezocomposites are very attractive materials for transducers and biomedical application, due to its high electromechanical coupling effects. Reliability study on 1-3 piezocomposites subjected to cyclic loading condition in transducer application is one of the primary concern. Hence, this study focuses on 1-3 piezocomposites for various PZT5A1 fiber volume fraction subjected to electrical fatigue loading up-to  $10^6$  cycles and at various elevated temperature. Initially experiments are performed on 1-3 piezocomposites, in order to understand the degradation phenomena due to various range in amplitude of electric fields (unipolar & bipolar), frequency of applied electric field and for various ambient temperature. Performing experiments for high cycle fatigue and for different fiber volume fraction of PZT5A1 is a time consuming process. Hence, a simplified macroscopic uni-axial model based on physical mechanisms of domain switching and continuum damage mechanics has been developed to predict the non-linear fatigue behaviour of 1-3 piezocomposites for temperature dependent electrical fatigue loading conditions. In this model, damage effects namely domain pinning, frozen domains and micro cracks, are considered as a damage variable ( $\omega$ ). Remnant variables and material properties are considered as a function of internal damage variable and the growth of the damage is derived empirically based on the experimental observation to predict the macroscopic changes in the properties. The measured material properties and dielectric hysteresis (electric displacement vs. electric field) as well as butterfly curves (longitudinal strain vs. electric field) are compared with the simulated results. It is observed that variation in amplitude of bipolar electric field and temperature has a strong influence on the response of 1-3 piezocomposites. © 2016 Author(s). All article content, except where otherwise noted, is licensed under a Creative Commons Attribution (CC BY) license (<http://creativecommons.org/licenses/by/4.0/>). [<http://dx.doi.org/10.1063/1.4944582>]

### I. INTRODUCTION

Piezoelectric materials are a class of smart materials, which play a major role in design of sensors and actuators. Though, we have numerous choice of piezoelectric materials, lead zirconate titanate (PZT) is preferred for transducer applications due to its high electromechanical coupling and response at higher frequencies(MHz).<sup>1</sup> Piezoelectric materials exhibit linear response for low external fields. However, it exhibits non-linear behavior for higher electric field and/or stresses. Non-linearity in PZT is caused mainly due to reorientation of domains in micro-structure, which is referred as domain switching.<sup>2</sup> Though, many literature reports about the non-linear behavior of PZT, its reliability in industries is the most concerned problem. The reliability of PZT transducers is influenced by four major mechanisms of damage such as aging, fatigue, micro-cracks and dielectric breakdown. Among these, fatigue due to cyclic loading seems to be more fatal.<sup>3</sup> Since

---

<sup>a</sup>Electronic address: [mohanry90@gmail.com](mailto:mohanry90@gmail.com)

<sup>b</sup>Electronic address: [aarajan@iitm.ac.in](mailto:aarajan@iitm.ac.in)

in most of the applications, piezoelectric materials are not only subjected to intermittent varying high or low external loads, it will also be subjected to continuous external fields during operation. Generally, fatigue in piezoelectric materials leads to reduction of switchable polarization and the degradation of electromechanical coupling factors.<sup>4</sup> Fatigue tests conducted on PZT showed that the material undergoes significant degradation even at ambient temperature, and the degradation depends on the magnitude and rate of applied electric field.<sup>5-7</sup> The increase in number of cycles of the applied electric field, not only leads to macroscopic cracking and dielectric breakdown, but it also degrades the macroscopic material properties.<sup>8</sup> Observed degradation in material properties and switchable polarization are caused due to microscopic changes namely domain pinning, dielectric layers near the electrode and frozen domains (non-switchable domains), etc.<sup>9-12</sup> Besides the experimental studies, a number of theoretical models have been developed to study the degradation caused in materials due to fatigue loading condition. These models are based on macro-micro mechanical approach, wherein the observed degradation are modeled by considering the microscopic change as the internal variable.<sup>13</sup> Technological advancements in the sensors and actuators show that, piezocomposites are more efficient than bulk PZT in biomedical, underwater and energy harvesting application due to its superior properties.<sup>14</sup> A variety of piezocomposite materials can be made by combining piezoceramic elements with a passive polymer (epoxy) or active polymer. The optimum configuration which gives the higher electromechanical coupling factor are selected by studying various topology. One popular type configuration is 1-3 piezocomposite, which contains piezoelectric rods of one dimension embedded in a polymer matrix of three dimensions and aligned along the thickness direction.<sup>15</sup> Nowadays, bulk piezoelectric materials are replaced with 1-3 type piezocomposites, since the bulk PZT are stiff and the lack of flexibility can cause premature failure in their applications. The tailor made properties in piezocomposites enable us to use them in bio-medical transducers, underwater applications, micro positioning systems and vibration suppression,<sup>16</sup> wherein these materials are subjected to high loading conditions,<sup>17</sup> Though 1-3 piezocomposites are already used in many industrial applications, it is necessary to understand its reliability.<sup>18</sup> The reliability study in 1-3 piezocomposites is more complex since the interaction of passive polymer and active PZT comes into account.<sup>19</sup> In the literature, studies about 1-3 piezocomposites are focused on the variation of material properties as function of volume fraction of PZT fiber and to identify the effective material properties and influence of fiber orientation using analytical approach.<sup>20-22</sup> Non-linear behavior of 1-3 piezocomposites are studied by subjecting it to various loading conditions above the coercive electric field, which shows that the fiber volume fraction dependency in the switching polarization, and remnant values.<sup>23</sup> Various applications studies were also carried out to find out the performance when compared to the bulk PZT.<sup>24-26</sup> Electrical fatigue loading on 1-3 piezocomposites for high bipolar electric field shows the strong dependence on the degradation of material properties for various volume fraction of PZT fiber. The damages are more for decreasing fiber volume fraction which results in deterioration of material performance.<sup>27</sup>

In the literature, even-though few research work are reported about the fatigue studies of PZT, the authors are not aware of detailed work in determining the performance behaviour of 1-3 piezocomposites subjected to electrical fatigue loading and at elevated temperature. Hence, it is mandate to study the performance of 1-3 piezocomposites, for repeated cyclic electric field up-to  $10^6$  cycles for different ambient temperatures. In this work, initial fatigue experiments are performed for various loading amplitude (unipolar, bipolar and bipolar at below  $E_c$ ), to understand the maximum deterioration effects. Fig. 1 shows that measured data on the performance behavior of 1-3 piezocomposites. It is observed that there is a significant reduction in performance subjected to higher bipolar electric field. Based on the initial experiments, this work is extended to perform electrical fatigue experiments for various fiber volume fractions of PZT5A1( $v_f$ ) and is also focused to understand the deterioration effects under elevated thermal loading condition. Performing experiments for large number of loading cycles and different fiber volume fraction will be costly affair and time consuming process. Hence an attempt has been made to develop an analytical model wherein damage parameter is introduced as a cumulative effect (micro-crack, domain pinning, frozen domains, etc). Simulated results based on the model for 1-3 piezocomposites with different volume fractions are compared with the measured data.

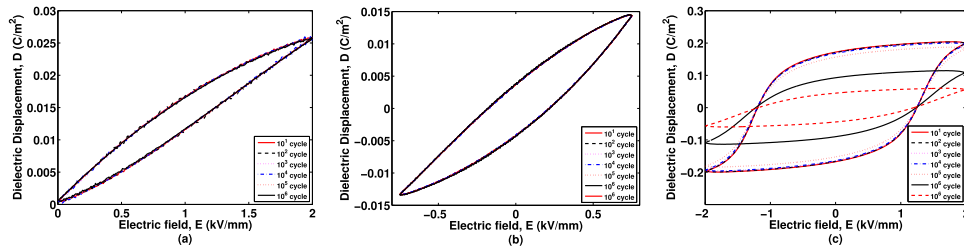


FIG. 1. Experimental results showing the Electrical fatigue results for 65% PZT5A1 fiber exposed to  $50^\circ C$  Isothermal temperature (a) Unipolar 0 to 2  $kV/mm$  (b) Bipolar at  $\pm 750 V/mm$  (c) Bipolar at  $\pm 2 kV/mm$ .

## II. EXPERIMENTAL DESCRIPTION OF TEMPERATURE DEPENDENT ELECTRICAL FATIGUE

Fatigue Experiments are performed on 1-3 piezocomposites & bulk piezoceramics samples subjected to cyclic electric field at elevated temperatures. Commercially available poled 1-3 piezocomposites (smart material corporation, Germany) and bulk piezoceramics (Ceramtec, Germany) are used for measurements. In 1-3 piezocomposites, three different volume fraction of PZT5A1 fiber constituents namely; 80% (800  $\mu m$  fiber diameter), 65% (250  $\mu m$  fiber diameter) and 35% (105  $\mu m$  fiber diameter) are used.

**Cyclic Loading:** Preliminary tests has been carried on these samples to understand its performance degradation, subjected to different amplitude of electrical loading ( $\pm 750 V$ , 0 to 2  $kV$ ,  $\pm 2 kV$ ) and various loading rates (0.1 – 100 Hz); see Fig. 1. Based on this study, it is decided to perform fatigue experiments under bipolar electric field with an amplitude of  $\pm 2 kV/mm$  at frequency of 50 Hz. The loading conditions are chosen based on the dielectric breakdown of the material and maximum loading condition. All the samples are cycled up-to  $10^6$  cycles and subjected to various operating temperatures (Room Temperature ( $\approx 27^\circ C$ ),  $50^\circ C$ ,  $75^\circ C$  and  $100^\circ C$ ). Measurements are restricted up-to  $100^\circ C$ , since the average glass transition temperature of epoxy polymer is around  $125^\circ C$ .

**Experimental setup:** A triangular waveform at 50 Hz frequency is generated by using function generator (Tektronix AFG3022B). The generated signal is amplified by high voltage amplifier (TREK PD05034) to  $\pm 2 kV$ . The amplified voltage is supplied to the upper electrode of the specimen and the bottom electrode is connected to brass, which in-turn connected in series with a known reference capacitor ( $C_r = 10 \mu F$ ) and the ground for charge measurement based on the modified Sawyer-Tower circuit. The voltage drop across(V) the capacitor is measured using high input impedance electrometer (Keithley 6517B) which is used to calculate the dielectric displacement (D). The longitudinal strain induced by electric field is measured using a laser-vibrometer (Polytec NLV-2500) with a resolution of 0.015 nm. All input and measured data are recorded with DAQ card (NI 9215) using LabVIEW. To isolate the external vibrations, the entire setup is placed over the vibration isolation table (Holmarc) while performing experiments. The specimen holder is designed specially to perform experiments under temperature dependent electrical fatigue loading. In order to provide uniform heating, ring type heater is used in the holder. Silicon oil of 32  $kV$  dielectric strength is used to avoid arcing at elevated electric field and temperature. A closed control loop with PID controller (Shimax MAC5D) and K type thermocouple (placed on top of the heater) is used to control/maintain the temperature on the heating element. A non-contact type IR thermal sensor (ThermoMETER-CT-M3, micro-epsilon) is used to measure the temperature variation on the sample. The specimens are heated to the required temperature and the dwell period is maintained to attain the thermal equilibrium. All the measurements are carried out along the thickness direction. The above experimental procedure is done initially at room temperature for one set of specimens and then the procedure is repeated for  $50^\circ C$ ,  $75^\circ C$  and  $100^\circ C$ .

**Measurements of material properties:** The D-Meter (Concord Ceramics, India) is used to measure piezoelectric coefficients ( $d_{33}$ ), which works on the principle of berlin court measurement. The dielectric permittivity ( $\kappa_{33}$ ) is measured based on high field method wherein samples are subjected to unipolar loading condition (0 – 1  $kV/mm$ ), and the slope of unloading region is used. Mechanical (compressive loading) experiments are performed to measure the elastic compliance ( $C_{33}$ ) and the

data shows that variation of compliance is minimal as a function of cyclic loading, since stiffness of the material has least effect due to repeated domain switching.<sup>28</sup> In order to measure the degradation parameters, measurements are made at specific intervals of cycles ( $10^1$ ,  $10^2$ ,  $10^3$ ,  $10^4$ ,  $10^5$  &  $10^6$ ). The experiments are repeated for 3 sets of samples and the averaged data is considered for the analysis.

### III. TEMPERATURE DEPENDENT UNI-AXIAL FATIGUE MODEL

The experimental measurements on fatigue behavior for various fiber volume fractions and different environmental conditions is laborious and time consuming process. Based on the experimental observations, a simple fatigue model has been proposed to simulate the effect of fatigue loading cycles. This analytical model can be used to predict the fatigue behaviour of 1-3 piezocomposites for various fiber volume fraction, different operating temperature and range of frequencies. The generalized nonlinear electro-mechanical constitutive relation can be written as:

$$D_i = \kappa_{ijkl} E_j + d_{ijkl} \sigma_{kl} + P_i^r \quad \text{and} \quad \epsilon_{ij} = S_{ijkl} \sigma_{kl} + d_{kij} E_k + \epsilon_{ij}^r \quad (1)$$

Where  $\sigma_{kl}$ ,  $\epsilon_{ij}$ ,  $D_i$  and  $E_i$  are the stress tensor, strain tensor, electric field vector and electric displacement vector respectively.  $S_{ijkl}$ ,  $d_{kij}$  and  $\kappa_{ij}$  are the elastic compliance tensor, piezoelectric tensor and dielectric permittivity tensor respectively.

**Physical approximation of a uni-axial model:** Piezoelectric materials exhibit electro-mechanical coupled phenomena since the crystal structure lacks a center of symmetry. Above the Curie temperature ( $T_c$ ), it is referred as paraelectric state and the crystal structure of the unit cell is cubic and centro-symmetric. In paraelectric phase, the relative atom positions in a cubic structure gives rise to a vanishing net dipole moment renders null piezoelectric effect. However, the operating temperature lowered down to below  $T_c$ , it undergoes a phase transformation from cubic to tetragonal or rhombohedral structure which is defined as ferroelectric phase. In this state, atomic positions in the crystal will change and give rise to nonzero net dipole moments is referred to as spontaneous polarization ( $P^s$ ). Movement of atomic positions in a lattice renders distortions consequently leading to mechanical strain as spontaneous strain ( $\epsilon^s$ ). In this model, a tetragonal structure is considered wherein the unit cell can orient in six different directions with respect to the crystallographic axes as shown in Fig. 2 and each of them is defined as a variant or a domain. Since experiments are performed under thickness (along poling direction) mode, a thermodynamically consistent uni-axial model<sup>29</sup> is extended to study the non-linear fatigue effects wherein six possible domain structures are simplified into three variants as two out-of-plane variants (Y and Y0) and one in-plane variant (i.e X, X0, Z and Z0). The three variants can be represented as 1, 2, 3, where 1 and 2 represents the out-of-plane variants; 3 represents the in-plane variant and their corresponding volume fractions are indicated as  $\Phi_1$ ,  $\Phi_2$  and  $\Phi_3$ ; refer fig 2.

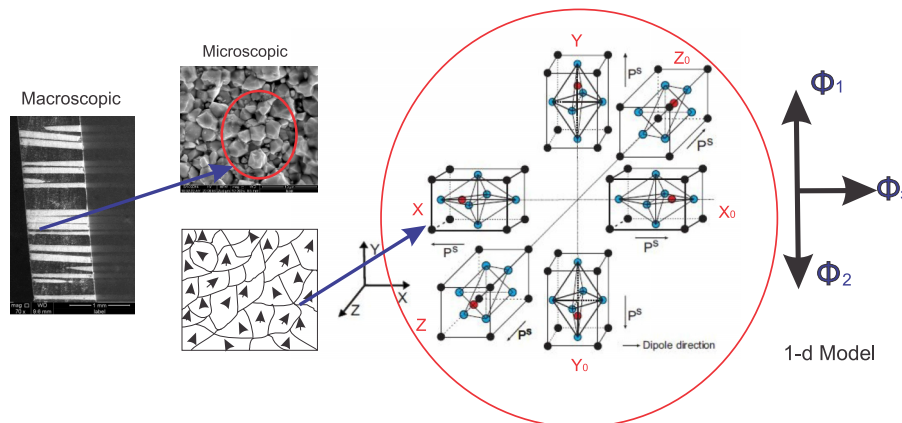


FIG. 2. Schematic representation of tetragonal crystal structure in the uni-axial model.

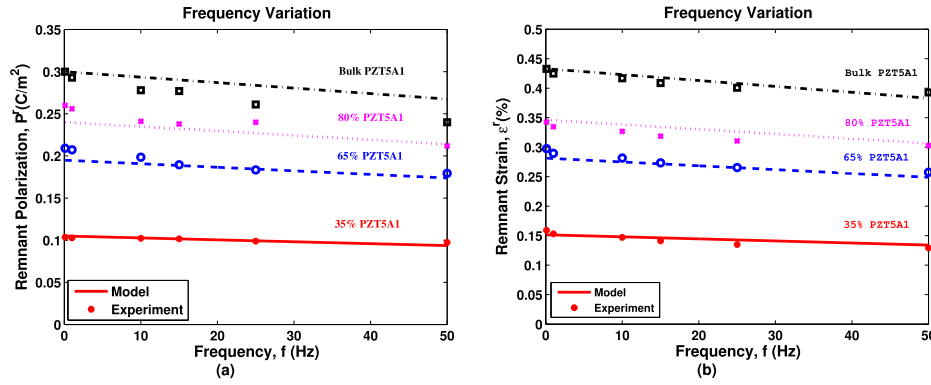


FIG. 3. Frequency dependency of (a) Remnant polarization-  $P^r(f)$  (b) Remnant Strain -  $\epsilon^r(f)$ .

**Frequency dependent material properties:** It is reported that the frequency of applied electric field influences the performance of piezoelectric materials.<sup>30</sup> Since 1-3 piezocomposite consist of passive polymer matrix, the loading frequency will have significant effects in the performance behaviour. In order to accommodate the frequency effects in the model, initial experiments are performed to measure the remnant polarization and strain as a function of input loading frequency: refer Fig. 8. Measured data shows that the remnant polarization and strain decrease linearly with increase in loading frequency (1 – 50 Hz); refer Fig. 3. Based on the observation, a linear expression has been introduced as shown in Eq. (2).

$$P^r(f) = \nu_f(c_{fp} \cdot f + p^{r0}) \quad \text{and} \quad \epsilon^r(f) = \nu_f(c_{f\epsilon} \cdot f + \epsilon^{r0}) \quad (2)$$

where  $\nu_f, f, c_{fp}$  and  $c_{f\epsilon}$  are the fiber volume fraction, frequency of the applied electric field, frequency constant for remnant polarization and remnant strain respectively.  $p^{r0}$  and  $\epsilon^{r0}$  are considered as the initial/reference remnant polarization and strain, which is measured at quasi-static loading (0.1 Hz). This expression is also extended for 1-3 piezocomposite with various fiber volume fraction. From the literature,<sup>31</sup> it is observed that the rate effects are fitted with linear approximation as a function of volume fraction of domain switching variants and loading frequency.

**Temperature dependent material properties:** Operating temperature on PZT plays certainly an important role in the response. Influence of temperature on material properties and remnant quantities of PZTs are well understood under electrical loading conditions.<sup>32-34</sup> In this work, an attempt has been made to evaluate the temperature dependence in the material properties and remnant quantities for 1-3 piezocomposites. Based on the observation, an linear expression has been introduced as shown in Eq. (3).

$$P^r(\theta, f) = P^r(f) \cdot \left(1 - \frac{\alpha_\theta \cdot \Delta\theta}{\nu_f}\right) \quad \text{and} \quad \epsilon^r(\theta, f) = \epsilon^r(f) \cdot \left(1 - \frac{\alpha_\theta \cdot \Delta\theta}{\nu_f}\right) \\ \kappa_{33}(\theta) = \kappa_{33} \cdot \left(1 + \frac{\alpha_\theta \cdot \Delta\theta}{\nu_f}\right) \quad \text{and} \quad d_{33}(\theta) = d_{33} \cdot \left(1 + \frac{\alpha_\theta \cdot \Delta\theta}{\nu_f}\right) \quad (3)$$

where  $\nu_f, f$  and  $\alpha_\theta$  are the fiber volume fraction, frequency of the applied electric field and temperature dependent constant respectively.  $P^r(f)$  and  $\epsilon^r(f)$  are the remnant polarization and remnant strain for that corresponding frequency of the applied electric field.  $\kappa_{33}$  and  $d_{33}$  are the dielectric permittivity and piezo-electric coupling coefficient at room temperature ( $\approx 27^\circ\text{C}$ ). Fig. 4 shows the comparison of experimental and theoretical prediction on temperature dependent remnant quantities which shows comparable correlation. Similarly, temperature dependent dielectric constant ( $\kappa_{33}$ ) and ( $d_{33}$ ) are compared with the measured data from the literature<sup>33</sup> as shown in Fig. 5.

**Damage dependent material properties:** In piezoelectric materials (PZT) during repeated cyclic loading, damage is caused due to internal factors such as domain wall pinning, frozen domains, coalescence of point defects, agglomeration of defects and micro cracks.<sup>4,35</sup> Hence, degradation of

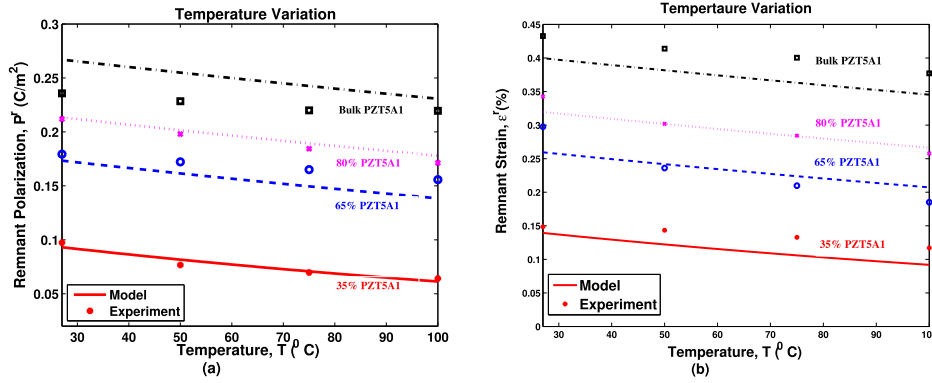


FIG. 4. Temperature dependency of (a) Remnant polarization -  $P_r(\theta, f)$  (b) Remnant Strain -  $\epsilon_r(\theta, f)$ .

material properties are due to the development of internal damage. From the modeling prospective, it is best practice to approximate as a single variable rather quantifying many internal factors, since damage is a cumulative effect in composites. In the present paper, the variation in material properties is formulated as a material function of the damage variable based on continuum damage mechanics. In the present model damage variable is considered as a linear function of material properties and these simplifications are made to reduce the number of constants evaluation. The material properties and remnant quantities as a function of damage parameter are represented as:

$$\begin{aligned} P^r(\theta, f, \omega) &= (1 - \omega) \cdot P^r(\theta, f) \quad \text{and} \quad \epsilon^r(\theta, f, \omega) = (1 - \omega) \cdot \epsilon^r(\theta, f) \\ \kappa_{33}(\theta, \omega) &= (1 - \omega) \cdot \kappa_{33}(\theta) \quad \text{and} \quad d_{33}(\theta, \omega) = (1 - \omega) \cdot d_{33}(\theta) \end{aligned} \quad (4)$$

where  $\omega$ ,  $P^r$ ,  $\epsilon^r$ ,  $\kappa_{33}$ ,  $d_{33}$  denote damage variable, initial remnant polarization, remnant strain, dielectric permittivity and piezo-electric coupling coefficient, respectively.

**Switching Criteria:** Domain switching is the main cause for the non-linear (hysteretic) effects in ferroelectric materials. Numerous modeling methods based on macro and micro-mechanical approaches were reported in literature. In this work, a thermodynamically consistent approach<sup>36</sup> is extended for a uni-axial loading conditions. Based on the assumptions of isothermal processes, homogeneous temperature fields and Clausius-Duhem inequality conditions, the generalized dissipation inequality can be expressed as

$$[\sigma : \dot{\epsilon}^r + E \cdot \dot{P}^r] \geq 0 \quad (5)$$

Where  $\sigma$  - applied stress,  $E$  - applied electric field,  $P^r$  - remnant polarization,  $\epsilon^r$  - remnant strain and  $(\dot{\cdot})$  - defines time derivatives. Considering the switching process as quasi static a super-scripted dot ( $\dot{\cdot}$ ) over a variable can be replaced by an incremental quantity  $\Delta$ , the transformation strain and

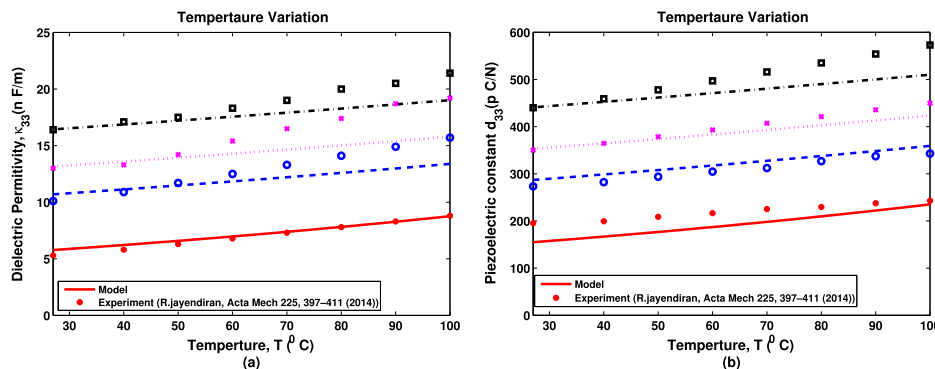


FIG. 5. Temperature dependency of (a) dielectric permittivity,  $\kappa_{33}(\theta)$  (b) piezo-electric coupling coefficient,  $d_{33}(\theta)$ .

displacement or polarization yields

$$\dot{P}^r = \Delta P_{\phi_i \rightarrow \phi_j}^r = \Delta P_{\phi_i}^r - \Delta P_{\phi_j}^r \quad \text{and} \quad \dot{\epsilon}^r = \Delta \epsilon_{\phi_i \rightarrow \phi_j}^r = \Delta \epsilon_{\phi_i}^r - \Delta \epsilon_{\phi_j}^r \quad \text{where } i = 1, 2, 3 \text{ \& } j = 1, 2, 3. \quad (6)$$

The driving force ( $f_{ij}$ ) (domains to switch from one state to another state) due to external applied loading conditions are derived, by substituting Equ. (4) and (6) in Eq. (5). In fatigue loading conditions, the domains are subjected to continuous switching. However, after certain loading cycles, the switching process will be limited, due to the frozen domains and micro-cracks in the micro-structure, which results in the reduction of macroscopic polarization and strain. In this model, it is considered as degradation in driving force which is function of damage ( $\omega$ ), frequency ( $f$ ) and temperature ( $\theta$ ) as follows:

$$f_{ij} = E \Delta P_{\phi_i \rightarrow \phi_j}^r(\theta, f, \omega) \quad (7)$$

The driving force will be calculated based on the above conditions for the present state of the domains and it will be compared with the critical (threshold) value for the possible switchable states.

$$f_{ij} \geq f_{cr180}, f_{cr90} \quad (8)$$

where  $f_{cr180}$ ,  $f_{cr90}$  are the critical energy barrier for  $180^\circ$  and  $90^\circ$  switching conditions. In this uni-axial model, there are two possibilities of  $90^\circ$  domain switching ( $\phi_1 \Leftrightarrow \phi_3$ ,  $\phi_2 \Leftrightarrow \phi_3$ ) and a  $180^\circ$  domain switching ( $\phi_1 \Leftrightarrow \phi_2$ ) are considered and compared.

$$f_{cr180} = 2P^r(\theta, f, \omega)E_{cr}(\theta, f, \omega) \quad \text{and} \quad f_{cr90} = P^r(\theta, f, \omega)E_{cr}(\theta, f, \omega) \quad (9)$$

**Damage evolution equation:** The evolution equation for the damage variable ( $\omega$ ) is used to describe the growth of the damage on the basis of continuum damage mechanics.<sup>35,37,38</sup> In the present paper, an evolution equation for the damage variable is formulated based on experimental results. Damage in 1-3 piezocomposites are influenced by switching process, hence switching criteria forms as the consistent condition for the damage. The exponential variation in damage are empirically formulated by using damage dependent parameters such as failure cycles ( $N_f$ - 90% degradation of its material properties and remnant quantities), coercive electric field ( $E_c$ ), maximum and minimum applied electric field ( $E_{max}$  &  $E_{min}$ ), volume fraction of PZT fiber ( $\vartheta_f$ ) and damage hardening parameters ( $A$  and  $m$ ) respectively.

$$\omega = A \left( \exp \left[ -m \frac{N_f}{N} \frac{E_c}{E_{max} - E_{min}} \vartheta_f \right] \right) \quad \text{for } f_{ij} \geq f_{cr} \quad (10)$$

The effect of frequency, temperature internal damage is introduced into the constitutive equations Eq. (11) by using the material functions instead of the material constants (Eq. (2), (3), and (4)). Generalized constitutive relation (Eq. (1)) can be reduced to a uni-axial electrical loading as

$$D_3 = \kappa_{33}(\theta, \omega) E_3 + P_3^r(\theta, f, \omega) \quad \text{and} \quad \epsilon_{33} = d_{33}(\theta, \omega) E_3 + \epsilon_{33}^r(\theta, f, \omega) \quad (11)$$

1000 grains (representation of a unit cell) are considered for the simulation and macroscopic quantities are calculated based on Reuss approximation technique.<sup>33</sup> The material properties considered for this Uni-axial fatigue model are listed in Table I. Figs. 6 and 7 show the macroscopic dielectric displacement and strain for 35 % of fiber volume fraction as function of number of cycles. It is observed that there is gradual decrease in dissipation of energy until  $10^4$  cycles. Further increase in

TABLE I. Material parameters used in Simulation for Uni-axial temperature dependent fatigue model.

Material	$S_{33}$ (GPa)	$\kappa_{33}$ (nF/m)	$d_{33}$ (pC/N)	$c_{fp}$ (C-sec/m <sup>2</sup> )	$c_{f\epsilon}$ (1/sec)	$\alpha_\theta$ (1/ <sup>0</sup> C)	$A$	$m$
PZT5A1	116.8	16.4	440	0.00065	0.001	0.00163	0.20	0.9
Epoxy	3.9	0.04	0	0	0	0	0	0

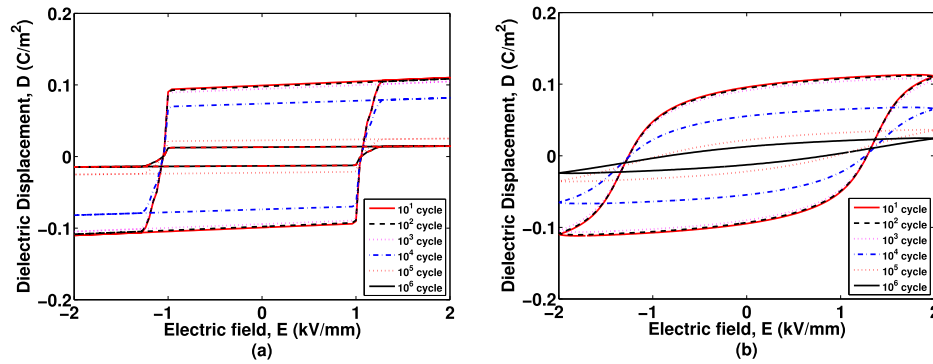


FIG. 6. Dielectric Hysteresis as a function of no of cycles (a) Uni-axial fatigue model (b) experimental results for 35% PZT5A1 at  $27^{\circ}\text{C}$ .

number of cycles ( $10^4$  to  $10^6$ ) it shows a rapid decrease in dissipation of energy, which results in hysteresis loops are get flattened. Simulated results are compared with the measured data, which is able to predict qualitatively the hysteresis area, remnant polarization and strain as function of cycles. This model can be used to identify qualitatively for higher fatigue cycles ( $10^7$  or  $10^8$ ) without performing experiments for long durations and also for various fiber volume fraction. Further research will be focused on development micro-mechanical model based on the fatigue mechanism.

#### IV. RESULTS AND DISCUSSION

Experiments are conducted on poled samples of 1-3 piezocomposites. The tests were carried out at different elevated temperatures upto  $10^6$  cycles, for various volume fractions of PZT5A1 fiber ( $v_f$ ). Initial experiments for various amplitudes of electrical loading, show that maximum deterioration occurs above the coercive electric field ( $E_c$ ); refer Fig. 1. Hence, in this work experiments are performed under electrical fatigue with bipolar electric field (amplitude beyond the coercive electric field ( $E_c$ )), at elevated temperatures. The material properties such as dielectric permittivity ( $\kappa_{33}$ ), and piezoelectric constant ( $d_{33}$ ) are measured by using an impedance analyzer (Wayne Kerr 6505B) and D-meter (Concord ceramics) based on IEEE standards.<sup>39</sup> Temperature dependent electrical fatigue behaviour of 1-3 piezocomposites is measured by following the procedures as described in Section II.

Fig. 8 shows the measured rate dependency (0.1 – 50 Hz) for 35% PZT5A1 fiber volume fraction. It shows that the rate of the applied electric field increases with decrease in hysteresis and butterfly loop area, which in-turn gradually reduces the remnant polarization and strain. As frequency increases, there is an increase in coercive electric field ( $E_c$ ), which depicts that the complete

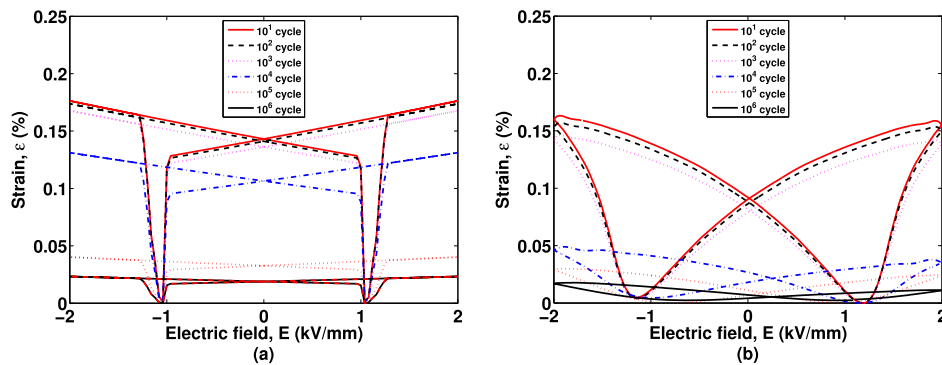


FIG. 7. Strain Hysteresis as a function of no of cycles (a) Uni-axial fatigue model (b) experimental results for 35% PZT5A1 at  $27^{\circ}\text{C}$ .

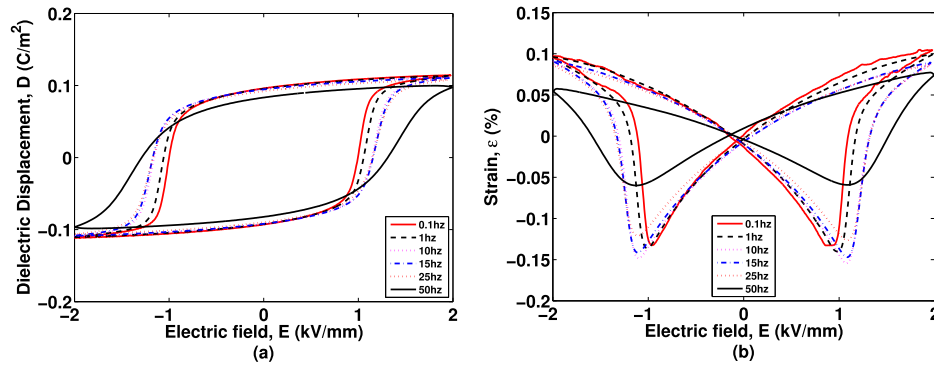


FIG. 8. Rate effects for 35% PZT5A1 (a) Dielectric Hysteresis (b) Strain Hysteresis.

domain switching occurs at lower loading rate than the higher rates. It is obvious that the required time for the domains to switch may not be enough at high loading rates. More pronounced rate effects are observed in strain behavior due to the necessity of high electric field for the saturation. However, the available electrical input is limited that renders reduction in the amplitude of overall strain.<sup>33,40-44</sup>

The non-linear fatigue behaviour of 1-3 piezocomposite is measured for cyclic bipolar electric field with an amplitude beyond the coercive (critical) electric field ( $E_c$ ) at three different temperature ( $50^{\circ}C$ ,  $75^{\circ}C$  and  $100^{\circ}C$ ): refer Figs. 9 & 10. It is evident from the results that the dielectric displacement ( $D$ ) of piezocomposite samples reduces with increase in PZT fiber volume fraction. This is due to the fact that epoxy matrix renders passive contribution to the applied electric field. Dielectric Hysteresis shows that with increase in operating temperature and number of cycles, the area under the loop decreases and it gets flattened at later stage of cyclic load. One reason could be that the available free energy within the domains (unstable state) are high at higher temperatures. In order to attain the stable state, the domains tend to return to a state of lower potential and it reflects in the reduction of area under the dielectric loop at elevated temperature. Also, under high fatigue cycles, the agglomeration of point defects in the micro-structure (damage) reduces the resistance offered by the neighboring domains to a particular domain of interest (switching domain) that renders reduction in the performance behavior. In general, the bond between dipoles are flexible at elevated temperature that allows the dipoles free to move. This effect can be identified from the hysteresis loop that there is a reduction in macroscopic coercive field ( $E_c$ ) with increase in temperature and independent of loading cycles.

The variation of strain with respect to electric field (Butterfly loop) for 35% PZT5A1 volume fraction is shown in Fig. 10. Similar to the dielectric hysteresis loop, the loop area for the butterfly hysteresis loop tend to decrease with increase in temperature and number of cycles. At higher loading cycles and elevated operating temperatures, un-symmetric behavior in strain is observed. Strain amplitude in butterfly loop namely right wing ( $\Delta\epsilon^{rw}$ ) is higher than the left wing ( $\Delta\epsilon^{lw}$ ). Variation in amplitude of strain, renders the axis shift of butterfly loop towards positive field direction, which

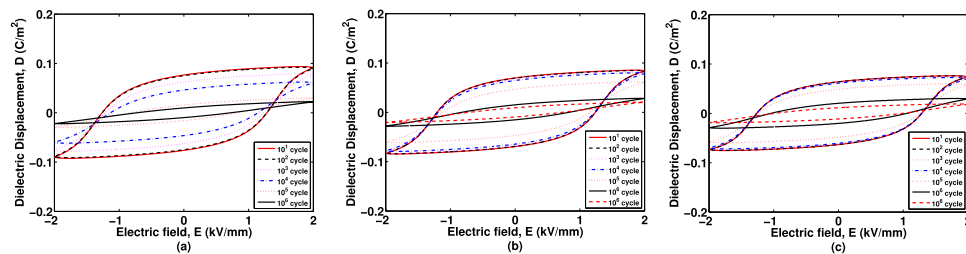


FIG. 9. Dielectric Displacement hysteresis results for 35% volume fractions of PZT5A1 at a)  $50^{\circ}C$  b)  $75^{\circ}C$  c)  $100^{\circ}C$  temperature.

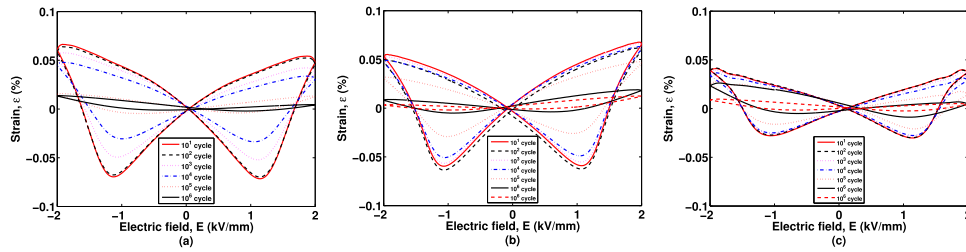


FIG. 10. Strain Hysteresis results for 35% volume fractions of PZT5A1 at a) 50°C b) 75°C c) 100°C temperature.

is referred as asymmetry. The asymmetry phenomenon is predominant as a function of fatigue cycle and operating temperature. Similar observation of strain asymmetry in fatigue studies are reported in literature.<sup>45,46</sup> In cyclic loading, the asymmetry in the strain observed might be due to the following reasons: fraction of previously switchable domains are frozen-in in a particular direction (Switching process is not happening continuously subjected to cyclic loading) and the internal bias field restricts the applied electric field in a particular direction.

Fig 11, shows the simulated and experimental results of remnant polarization and amplitude of strain as function of the number of cycles for 35% volume fraction of PZT5A1 fiber( $v_f$ ). The observed results show that an increase in the number of cycles leads to a degradation in quantities that vary non-linearly. This shows good agreement with the simulated results which also vary in a similar manner. This non-linear behavior is replicated by all other volume fraction of PZT fiber. Upon experimenting at elevated temperatures, it was observed that an increased temperature leads to a slower rate of degradation ( $\frac{\Delta P_r}{P_r}$ ). The observed degradation shows a small offset from the simulated values in the amplitude of the right wing strain ( $\Delta \epsilon^{rw}$ ). This offset is due to the asymmetry in strain observed in the experiments, might be due to the model assumption of material properties directly proportional to the damage parameter. Fig 12, shows the measured material property values ( $d_{33}, \kappa_{33}$ ) compared with the simulated results. Observed degradation trends are similar to the remnant quantities, which is due to the domain switching process. Hence the damage is also coupled with the remnant and material properties. After  $10^6$  cycles the 1-3 piezocomposites degrade by almost 90% of its initial value. An increased temperature however, leads to a further degradation of the properties. The degradation observed shows a nominal decrease till  $10^4$  cycles. However, in between  $10^4$  to  $10^5$  cycles, the observed degradation is very high. The reason may be traced to the time taken to agglomerate the defects and frozen domains in the initial stage and once formed results in accelerated degradation of properties. Fig 13(a), shows the influence of damage for various loading amplitude of electrical field. The prediction shows that change in damage variable ( $\omega$ ) is negligible for unipolar or bipolar ( $< E_c$ ) loading conditions. It is obvious that domain switching effects may not occur under unipolar or lower bipolar electrical loading conditions. Fig. 13(b). shows the influence of damage for various fiber volume fraction

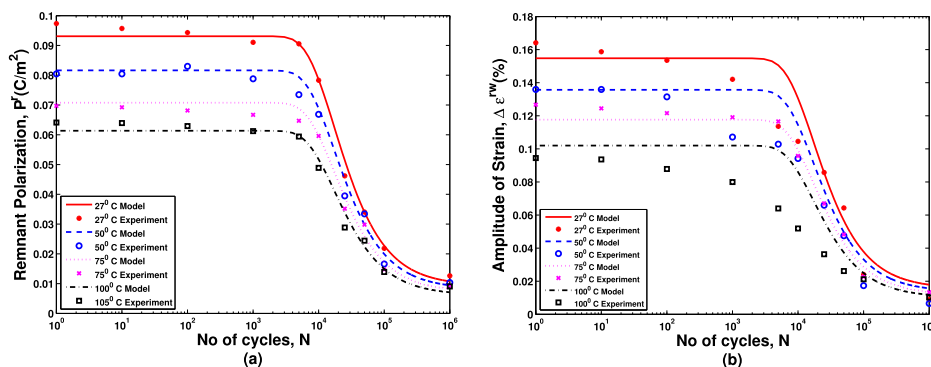
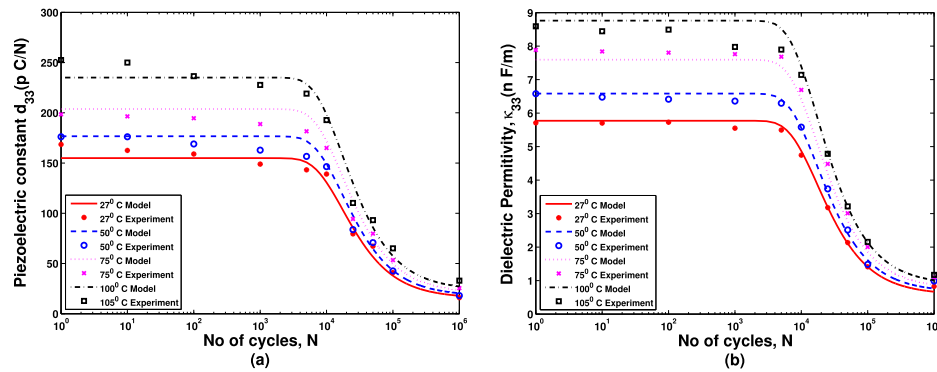
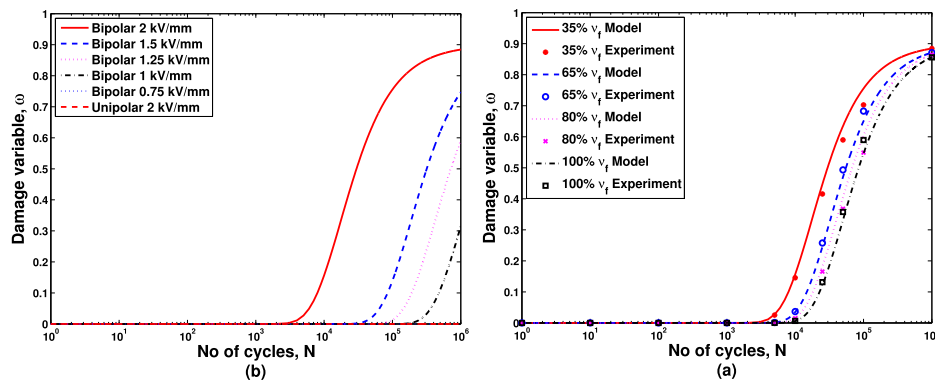


FIG. 11. Comparison of Model and Experiments for 35% PZT5A1 (a)  $P_r$  (b)  $\Delta \epsilon^{rightwing}$ .

FIG. 12. Comparison of Model and Experiments for 35% PZT5A1 (a)  $d_{33}$  (b)  $\kappa_{33}$ .FIG. 13. Damage variable( $\omega$ ) – (a) Influence of various loading amplitude of electrical field (b) Influence for bipolar ( $2kV/mm$ ) for various fiber volume fraction ( $v_f$ ).

at bipolar loading ( $2kV/mm$ ). Damage variable varies non-linearly (exponential) with increased number of cycles. There is significant difference in damage growth, as increase in fiber volume fraction. It is also observed that, the damage variable( $\omega$ ) saturates around  $10^6$  cycles. The developed model is found to replicate the nonlinear fatigue response of 1-3 piezocomposites obtained from the experimental results. Hence, the developed model can be used to predict the fatigue response for any combinations of fiber volume fractions. The output parameters obtained from this study will provide us the physical insight for device design using 1-3 piezocomposites. This model also helps to choose the appropriate fiber volume fraction based on the requirements of device design considering the fatigue effects.

## V. SUMMARY

Experiments are conducted to study the electrical fatigue behavior of 1-3 piezocomposites with different fiber volume fractions under elevated temperatures. Uni-axial fatigue model based on damage mechanics is proposed to evaluate the temperature dependent electrical fatigue behavior on 1-3 piezocomposites. The experimental observation shows that the maximum deterioration in material performance are caused due to repeated domain switching for higher amplitude of loading (above coercive electric field  $E_c$ ) and at elevated temperature. It is also observed that higher operating temperature influences the fatigue behaviour by reducing the degradation rate. Theoretical prediction of material properties degradation shows good agreement with experiment results. The model is able to predict the degradation in material properties and remnant quantities. Developed model is not able to take into account of grain boundary interaction effects and domain wall motion that renders the simulated results in qualitative agreement with measured data. Further research will be focused on the development of micro-mechanics based physical model for fatigue studies.

- <sup>1</sup> R. C. Smith, *Smart Material Systems-Model Development* (SIAM, Philadelphia, 2005).
- <sup>2</sup> J. E. Huber and N. A. Fleck, *European Journal of Mechanics A/Solids* **23**, 203 (2004).
- <sup>3</sup> D. Lupascu and J. Rödel, *Advanced Engineering Materials* **7**, 882 (2005), ISSN 1438-1656.
- <sup>4</sup> J. Nuffer, D. C. Lupascu, A. Glazounov, H.-J. Kleebe, and J. Rödel, *Journal of the European Ceramic Society* **22**, 2133 (2002), ISSN 09552219.
- <sup>5</sup> N. Su, Yu Lia, and G. J. Weng, *Acta Materialia* **87**, 293 (2015).
- <sup>6</sup> S. Kamposiri, S. Pojprapai, R. Yimnirunand, and B. Marungsri, *World Academy of Science, Engineering and Technology* **6**, 12 (2012).
- <sup>7</sup> C. Miclea, C. T. An, L. Amarande, M. Cioangher, C. F. Miclea, C. P. L. Avit, L. Trupina, C. T. Miclea, and C. David, *Romanian Journal Of Information Science and Technology* **10**, 243 (2007).
- <sup>8</sup> N. Balke, H. Kungl, T. Granzow, D. C. Lupascu, M. J. Hoffmann, and J. Rödel, *Journal of the American Ceramic Society* **3874**, 3869-3874 (2007).
- <sup>9</sup> J. Nuffer, D. C. Lupascu, and J. Ro, *Acta Materialia* **48**, 3783 (2000).
- <sup>10</sup> H. Wang, T. Matsunaga, H.-T. Lin, and A. M. Mottern, *Smart Materials and Structures* **21**, 025009 (2012), ISSN 0964-1726.
- <sup>11</sup> V. Y. Shur, A. R. Akhmatkhanov, I. S. Baturin, V. Y. Shur, A. R. Akhmatkhanov, and I. S. Baturin, *Journal of Applied Physics* **124111** (2013).
- <sup>12</sup> Y. Zhang and D. C. Lupascu, *Journal of Applied Physics* **100**, 054109 (2006), ISSN 00218979.
- <sup>13</sup> M. Okayasu, N. Odagiri, and M. Mizuno, *International Journal of Fatigue* **31**, 1434 (2009), ISSN 01421123.
- <sup>14</sup> K. Uchino, *Ferroelectric Devices* (Marcel Dekker, New York, 2000).
- <sup>15</sup> O. Sigmund, S. Torquato, and I. A. Aksay, *Journal of Materials Research* **13**, 1038 (2011).
- <sup>16</sup> W. Smith, in *[Proceedings] IEEE 7th International Symposium on Applications of Ferroelectrics* (1990), pp. 145–152.
- <sup>17</sup> H. J. Lee, S. Zhang, X. Geng, T. R. Shrout, H. J. Lee, S. Zhang, X. Geng, and T. R. Shrout, *Applied Physics letters* **101**, 253504, 253504 (2012).
- <sup>18</sup> M. Okayasu, G. Ozeki, and M. Mizuno, *Journal of the European Ceramic Society* **30**, 713 (2010).
- <sup>19</sup> C. B. V.Y.Topolov, *Electromechanical Properties in Composites Based on Ferroelectrics* (Springer, London, 2009).
- <sup>20</sup> C. w. Nan and G. J. Weng, *Journal of Applied Physics* **416** (2010).
- <sup>21</sup> W. Li-kun, L. Li, Q. Lei, W. Weiwei, and D. Tianxiao, *Journal of Applied Physics* **104**, 064120 (2008), ISSN 00218979.
- <sup>22</sup> R. Kar-Gupta and T. A. Venkatesh, *Journal of Applied Physics* **98**, 054102 (2005), ISSN 00218979.
- <sup>23</sup> R. Jayendiran and A. Arockiarajan, *Journal of Applied Physics* **112**, 044107 (2012), ISSN 00218979.
- <sup>24</sup> D. Li and K. Duan, *Ferroelectrics* **466**, 86 (2014), ISSN 0015-0193.
- <sup>25</sup> M. C. Ray and A. K. Pradhan, *Smart Materials and Structures* **15**, 631 (2006), ISSN 0964-1726.
- <sup>26</sup> M. Gall and B. Thielicke, *Acta Mechanica* **224**, 2529 (2013), ISSN 0001-5970.
- <sup>27</sup> Y. Mohan, R. Jayendiran, and A. Arockiarajan, *Proc. of SPIE* **9432**, 1 (2015).
- <sup>28</sup> M. Kosec, A. Levstik, V. Bobnar, Z. Kutnjak, and C. Filipic, *Journal of the European Ceramic Society* **19**, 1233 (1999).
- <sup>29</sup> R. Jayendiran and A. Arockiarajan, *J. Appl. Phys.* **112** (2012).
- <sup>30</sup> A. K. Tagantsev, I. Stolichnov, E. L. Colla, and N. Setter, *Journal of Applied Physics* **90**, 1387 (2001), ISSN 00218979.
- <sup>31</sup> S.-j. Kim and Q. Jiang, *Int. J. Solids Struct.* **39**, 1015 (2002).
- <sup>32</sup> M. S. Senousy, R. K. N. D. Rajapakse, and M. S. Gadala, *Acta Materialia* **57**, 6135 (2009), ISSN 1359-6454.
- <sup>33</sup> R. Jayendiran and a. Arockiarajan, *Acta Mechanica* **225**, 397 (2013), ISSN 0001-5970.
- <sup>34</sup> D. W. Ji, S.-j. Kim, D. W. Ji, and S.-j. Kim, *Journal of Applied Physics* **214109** (2014).
- <sup>35</sup> M. Mizuno, T. Nishikata, and M. Okayasu, *Smart Materials and Structures* **22**, 105002 (2013), ISSN 0964-1726.
- <sup>36</sup> A. Arockiarajan, S. M. Sivakumar, and C. Sansour, *Smart Materials and Structures* **19**, 015008 (2010), ISSN 0964-1726.
- <sup>37</sup> J. L. Chaboche, *Journal of Applied Mechanics* **55**, 59 (1988), ISSN 0021-8936.
- <sup>38</sup> P. Gerber, C. Kügeler, U. Ellerkmann, P. Schorn, U. Böttger, P. Gerber, C. Kügeler, U. Ellerkmann, P. Schorn, U. Böttger *et al.*, *Applied Physics Letters* **112908**, 28 (2005).
- <sup>39</sup> IEEE, ANSI/IEEE Std. **89**, 176 (1988).
- <sup>40</sup> A. Achuthan and C. T. Sun, *Acta Materialia* **57**, 3868 (2009), ISSN 1359-6454.
- <sup>41</sup> N. Zhang, L. Li, and Z. Gui, *J. Euro. Ceramic Soc.* **21**, 677 (2001).
- <sup>42</sup> A. Chaipanich, N. Jaitanong, and R. Yimnirun, *Ferroelectrics Letters Section* **36**, 59 (2009), ISSN 0731-5171.
- <sup>43</sup> R. Yimnirun, Z. Luo, and S. Pojprapai, *Electronics Letters* **48**, 1062 (2012), ISSN 0013-5194.
- <sup>44</sup> D. Wang, Y. Fotinich, and G. P. Carman, *Journal of Applied Physics* **83**, 5342 (1998), ISSN 00218979.
- <sup>45</sup> N. Balke, T. Granzow, and J. Rödel, *Journal of Applied Physics* **105**, 104105 (2009), ISSN 00218979.
- <sup>46</sup> L. Yu, S.-w. Yu, and X.-q. Feng, *Materials Science and Engineering A* **459**, 273 (2007).